

# A Differential Scanning Calorimetry Study of the Assembly of Hexadecylamine Molecules in the Nanoscale Confined Space of Silicate Galleries

Yuqin Li and Hatsuo Ishida\*

Department of Macromolecular Science and Engineering, Case Western Reserve University, Cleveland, Ohio 44106-7202

Received October 17, 2001. Revised Manuscript Received December 21, 2001

The intercalation process of hexadecylamine into bentonite and the fine structure of hexadecylamine in nanoscale confined space are studied by differential scanning calorimetry and X-ray diffraction. Intercalated amine exhibits multiple melting temperatures that are approximately 30 °C higher than the bulk amine, providing strong evidence that amine molecules assume ordered structures within silicate layers. Amine-packing density influences the interlayer fine structures of the amine as well as the stacking regularity of the silicate layers. With the further intercalation of polymer molecules, the ordered structure of amine is strongly influenced.

## Introduction

The study of nanocomposites has attracted extensive industrial and academic attention in the past 10 years. Clay is widely used in nanocomposite formation because of its special nanoscale parallel structure and low cost. However, to insert mostly hydrophobic polymer chains into the hydrophilic silicate layers, cationic surfactants, such as alkylamine compounds, are usually used to modify the surface properties of clay prior to mixing with polymer.<sup>1–3</sup> The combination of the hydrophobic nature of the surfactant and the stable, layered structures of the silicate sheets leads to unique physicochemical properties. The amine-treated clays have been referred to as “organoclay” or “organophilic-clay” and are widely used as nanocomposite precursors. Industrially, organoclays are also used as rheology controlling agents in paints, greases, and cosmetics.<sup>4</sup> In all these applications, the behavior and properties of the hybrids depend strongly on the structure and molecular environment of the organic interlayer. Therefore, understanding the amine intercalation process and the formed organo-clay structure is essential in many industrial applications. Moreover, the assembly of amine in the interlayer space of layered silicates can be regarded as a novel state of aggregates in a two-dimensional nanoscale space immobilized between the ultrathin inorganic layers. They represent an ideal model for fundamental studies of molecules in the nanoscale confined space.

Studies on the assembly of amine have been reported in the literature; however, the information obtained is limited due to the techniques used. For example, wide-angle X-ray diffraction has traditionally been used to

study the intercalation of amine and, thereafter, intercalation of polymer chains into the silicate layers.<sup>5–7</sup> However, X-ray diffraction can provide information only about the stacking structure of the silicate layers, i.e., the *d* spacing change upon intercalation. The structure information of amine is masked by the strong diffraction signal from the silicate layers. Several other techniques were used, however, for the muscovite mica which has a large surface area on which the orientation of the clay surface can be controlled. For example, layers of hexadecyltrimethylammonium<sup>8</sup> and dimethyldioctadecylammonium<sup>9</sup> ions were investigated by advancing contact angle measurements and X-ray photoelectron spectroscopy. The near-edge X-ray absorption fine structure spectroscopy was used to study the orientation of the alkyl chains in monolayers of amine chains.<sup>10</sup> Atomic force microscopy (AFM) images led to the assumption of a quasi-crystalline order of the alkyl chains.<sup>11</sup> Due to the small size, few characterization techniques are available for the study of amine structures in montmorillonite, although some attempts were made by Fourier transform IR spectroscopy (FTIR).<sup>12</sup> In this paper, differential scanning calorimetry (DSC) was used to study the interlayer structure of organoclay. The DSC measurements provide, for the first time, the direct information on the ordered structure of the organic interlayer as well as a means to relate the intercalated structure to the bulk state. Additionally, the combina-

(5) Lagaly, G. *Solid State Ionics* **1986**, *22*, 43.

(6) Kawasumi, M.; Hasegawa, N.; Kato, M.; Usuki, A.; Okada, A. *Macromolecules* **1997**, *30*, 6333.

(7) Klapayta, Z.; Fujita, T.; Iyi, N. *Appl. Clay Sci.* **2001**, *19*, 5.

(8) Chen, Y. L.; Chen S.; Frank, C.; Israelachvili, J. N. *J. Colloid Interface Sci.* **1992**, *153*, 244.

(9) Herder, P. C.; Claesson, P. M.; Herder, C. E. *J. Colloid Interface Sci.* **1987**, *119*, 155.

(10) Brovelli, D.; Caseri, W. R.; Hahner, G. *J. Colloid Interface Sci.* **1999**, *216*, 418.

(11) Tsao, Y.; Yang, S. X.; Evans, D. F.; Wennerstrom, H. *Langmuir* **1991**, *7*, 3154.

(12) Vaia, R. A.; Teukolsky, R. K.; Giannelis, E. P. *Chem. Mater.* **1994**, *6*, 1017.

\* To whom correspondence should be addressed. E-mail: hxi3@po.cwru.edu.

(1) Fukushima, Y.; Inagaki, S. *J. Inclusion Phenom.* **1987**, *5*, 473.

(2) Usuki, A.; Kawasumi, M.; Kojima, Y.; Okada, A. *J. Mater. Res.* **1993**, *8*, 1174.

(3) Vaia, R. A.; Giannelis, E. P. *Macromolecules* **1997**, *30*, 8000.

(4) Jones, T. R. *Clay Miner.* **1983**, *18*, 399.

tion of DSC and X-ray diffraction results leads to a unique conclusion on the relationship between the interlayer amine structure and stacking of silicate layers.

### Experimental Section

**Materials.** The montmorillonite used was Bentolite-L, from Southern Clay Products, with a cation-exchange capacity (CEC) of approximately 80 meq/100 g. It was dried in a vacuum oven at 120 °C for 48 h prior to use. Hexadecylamine with purity of 98% was purchased from Aldrich Chemical Co. The weight average molecular weight of poly(ethyl methacrylate) (PEMA) is  $M_w = 550\,000$ , and it was also purchased from Aldrich.

**Instruments and Methods.** There are two primary preparation methods for organoclay: ion exchange<sup>13</sup> and ion-dipole intercalation.<sup>14</sup> The latter was used in this experiment. Clays with various amine concentrations were physically mixed at room temperature before encapsulation in hermetically sealed, aluminum DSC pans. To explore the intercalation process, the sample in the DSC pan was used directly without any further treatment. Other samples were annealed at 120 °C for 40 min in an oven before the DSC scan to investigate the effect of the chain-packing density.

An ordinary DSC and temperature-modulated DSC (TMDSC) were performed using 2920 MDSC from TA Instruments Inc. Cooling and temperature modulation were accomplished with a liquid nitrogen cooling accessory. Dry nitrogen gas with a flow rate of 80 mL/min was purged through the DSC cell. For all DSC experiments, a heating rate of 3 °C/min was used unless otherwise specified. For the temperature modulation experiment, a temperature amplitude of  $\pm 1$  °C and period of 60 s were used. The temperature and heat flow were calibrated using water, indium, and zinc at 3 °C/min. The mixtures of clay with different amounts of amine annealed at 120 °C for 40 min were used for the wide-angle X-ray diffraction study, which was performed by a Philips XRG 3100 diffractometer with Cu K $\alpha$  radiation, using a scanning speed and step size of 0.06°/min and 0.01°, respectively.

### Results and Discussion

Figure 1 shows the DSC thermograms of bulk amine heating (curve A), as well as both heating and cooling processes for the mixture of clay with amine at a concentration of 5.18 CEC (curves B–D), as an example. This mixture represents one of the highest amine concentrations studied in this paper. In the first heating of the mixture, as shown in curve B, the endothermic transition at 46.0 °C is from the melting of amine, which is the same behavior as the bulk amine in curve A. A heavily overlapped exothermic peak, which is absent in the pure amine, however, appeared with the peak position at 47.0 °C (the peak position is obtained from the curve resolving result). Moreover, a few additional endothermic peaks appeared between 50 and 80 °C during the heating process. To eliminate the possibility that these additional thermal behaviors are caused by thermal history, a second heating, curve C, was run after the sample was cooled to room temperature. Interestingly, the bulk amine melting transition at 46 °C together with the overlapped exothermic peak completely disappeared, while the high-temperature endothermic transitions reappear in the second heating, with

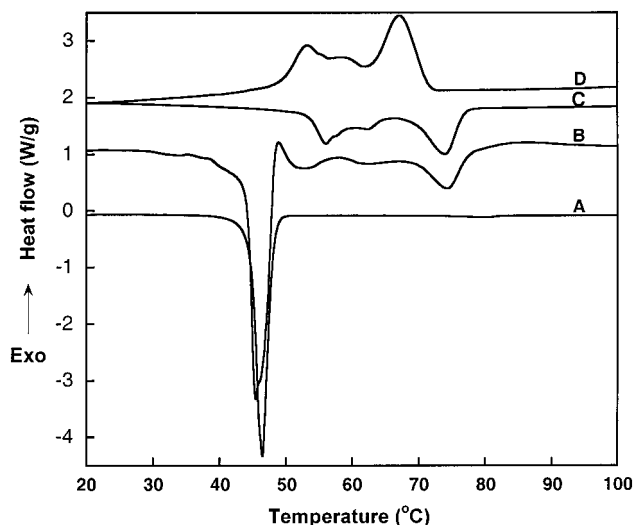


**Figure 1.** DSC curves for (A) pure hexadecylamine and (B) first heating, (C) second heating, and (D) cooling for the mixture of bentonite and amine with an amine concentration at 5.18 CEC. The thermograms were recorded with a heating rate of 3 °C/min and a cooling rate of 5 °C/min.

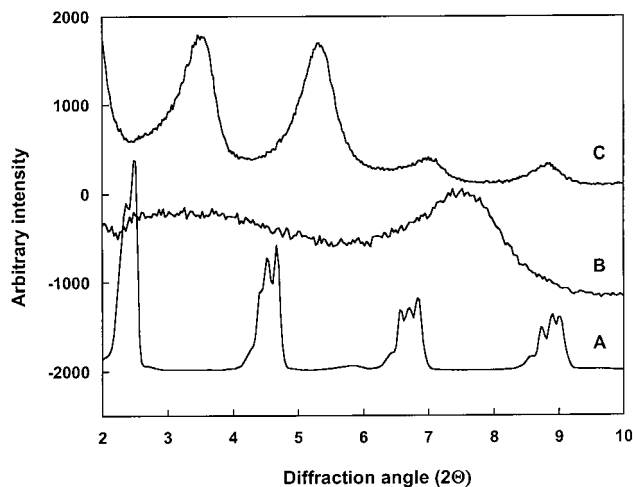


**Figure 2.** X-ray diffractograms of (A) pure hexadecylamine, (B) bentonite, and (C) mixture of bentonite and hexadecylamine with an amine concentration at 5.18 CEC, after the samples were annealed at 55 °C for 10 min.

little shift in peak temperature. Additional heating processes show no further change in the thermal behavior, which indicates that these high-temperature endothermic peaks are related to stable phase transitions. In the meantime, the correspondent exothermic peaks between 50 and 80 °C in the cooling process, curve D, which was done at a cooling rate of 5 °C/min, further confirm the notion of stable and thermoreversible phase transitions. Considering the high thermal stability of the clay below 180 °C, these few thermal transitions should come from the amine. Keeping in mind that the bulk amine melting transition shown in the first heating completely disappeared in the second heating, it is concluded that the structure of the amine changed during the heating process.

Figure 2 shows the X-ray diffractogram of the amine and clay mixture with amine concentration of 5.18 CEC, after annealing at 55 °C for 10 min. The diffractograms of the pure amine and the untreated clay are also shown as curves A and B as references. The diffraction from

(13) Okada et al. U.S. Patent 4,739,007, 1988.

(14) Lan, T.; Ying, L.; Beall, G. W.; Kamena, K. *Advances in Nanomer Additives for Clay/Polymer Nanocomposites*, Additives 99, San Francisco, CA, March 1999.

the original amine disappeared completely in the annealed mixture, curve C, as evidenced by the lack of diffraction at  $2\theta = 2.49$  and  $4.68^\circ$ . Although the signal from the confined amine is masked by the strong diffraction signal of the ordered structure of silicate layers, X-ray diffraction shows that the  $d$  spacing of the silicate layers is substantially increased by 3.91 nm. By combining the results from DSC and X-ray diffraction, we can conclude that the disappearance of the pure amine melting is caused by intercalation and that the stable, high-temperature endothermic transitions belong to the melting of the confined amine. Therefore, it can be further concluded that hexadecylamine forms ordered structures within the confined space of the silicate layers, and this nanoscale confined amine has melting temperatures much higher than the bulk amine. This phenomenon is analogous to the aliphatic side chain crystallization of liquid crystalline materials.<sup>15–17</sup> In the case of liquid crystalline materials, the main chain forms a parallel layered structure similar to the silicate layers with a gallery distance comparable to the silicate layers. In the meantime, the side chain forms an ordered structure, which is different from the free state crystal form, within the parallel layers. The difference between the case of organo-clay and liquid crystalline material is that the side chain of the liquid crystalline material has a chemical bond with the main chain, whereas the amine molecules do not have a strong permanent bond with the silicate surface. Nonetheless, the phenomenon that molecules form ordered structures different from their free state within the parallel nanoscale confined space is the same.

The difference in the melting temperature provides an easy way to distinguish the confined amine from the bulk amine. The fact that the bulk amine melting completely disappeared by the second heating process indicates that bulk amine no longer exists in this system. Since all of these thermal processes occur at relatively low temperature and under an inert atmosphere, thermal degradation of the amine can be ruled out. Hence, all the amine in the mixture is intercalated into the silicate layers, which means that clay can take much more amine than its cation-exchange capacity. Actually, the bulk amine melting transition does not appear in the second heating process until the amine concentration is around 7 CEC or above. Obviously, ion–dipole interaction is not the only driving force for the intercalation process. The van der Waals interaction among the amine chains and the tendency of close packing to form the ordered structure of the amine chains may contribute to further intercalation. A conclusion can be drawn that amine intercalates into the silicate layers immediately after its melting, because the order of these several processes should be: (i) bulk amine melting, (ii) amine intercalation, (iii) intercalated amine crystallization, and (iv) the melting of intercalated amine, and furthermore, the intercalated amine crystallization temperature is only  $1.0^\circ\text{C}$  higher than the bulk amine melting. The maximum temperatures

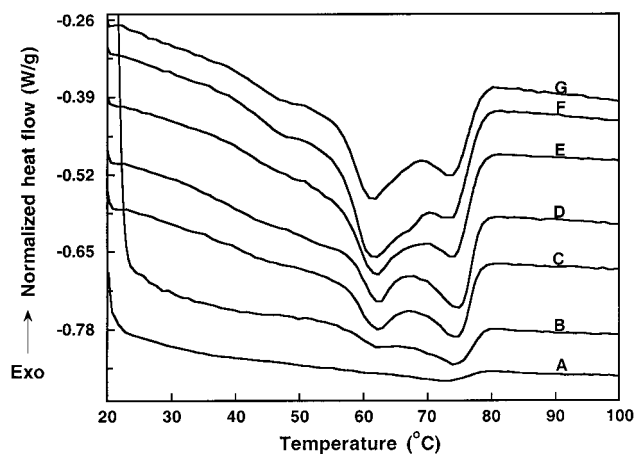


**Figure 3.** DSC thermograms for the mixtures of bentonite and hexadecylamine with amine concentrations at (A) 0.36, (B) 0.52, (C) 0.79, (D) 0.92, (E) 1.16, (F) 1.39, and (G) 1.59 CEC, at a heating rate of  $3^\circ\text{C}/\text{min}$ , after annealing at  $120^\circ\text{C}$  for 40 min.

for the bulk amine melting and the confined amine crystallization were obtained by curve resolving the heavily overlapped endothermic and exothermic peaks near  $46^\circ\text{C}$ . The apparent maximum temperature of the crystallization exotherm shifted toward higher temperature due to the heavy overlap of the two peaks. However, upon curve resolution, the temperature difference of these maxima is only  $1^\circ\text{C}$ . The small changes of the endothermic peak size and temperature between the first and second heating curves suggest that the amine molecules go through the redistribution and rearrangement processes after they are intercalated into the silicate layers. The high-temperature melting of the confined amine coincides well with the reversible  $d$  spacing change of the silicate layers between 60 and  $100^\circ\text{C}$ .<sup>18</sup> It is worth mentioning here that we did not observe any energy exchange for the intercalation process, despite attempting to detect such a transition at a high sensitivity. Whether the energy exchange is too small to be detected by the DSC or it is overlapped with the melting or crystallization process is not known at this stage.

The ordered structure of confined amine exists not only in the sample with very high amine concentration but also for the amine concentration as low as 0.36 CEC. For all the concentration ranges studied, the melting transition of the confined amine is observed. Figure 3 shows the DSC heating curves for samples with amine concentration from 0.3 to 1.6 CEC which were run after the samples were annealed at  $120^\circ\text{C}$  for 40 min. Y-axis is heat flow normalized to pure amine. Two broad melting transitions are observed, with peak temperatures at 62 and  $75^\circ\text{C}$ , respectively. The peak temperature remains constant for samples within this concentration range, while the relative intensity of these two transitions changes as a function of amine concentration. The influence of heating rate on the melting transitions is shown in Figure 4 for the sample with amine concentration at 0.92 CEC. Both melting transitions are shifted to higher temperatures as the heating

(15) Kricheldorf, J. H.; Domschke, A. *Macromolecules* **1996**, *29*, 1337.

(16) Hsu, W.-P.; Levon, K.; Ho, K.-S.; Myerson, A.; Kwei, T. K. *Macromolecules* **1993**, *26*, 1318.

(17) Lee, J. L.; Pearce, E. M.; Kwei, T. K. *Macromolecules* **1997**, *30*, 6877.

(18) Lerf, A. In *Handbook of Nanostructured Materials and Nanotechnology*; Nalwa, H. S., Ed.; Academic Press: New York, 2000; Vol. 5, p 127.



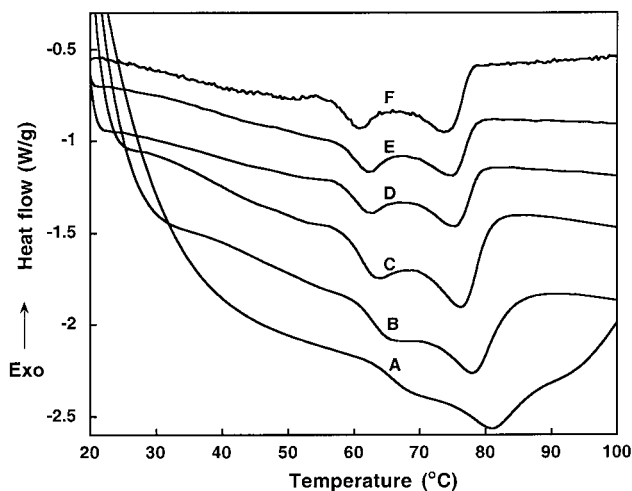


**Figure 4.** DSC thermograms for the mixture of bentonite and hexadecylamine with amine concentration at 0.92 CEC at heating rates of (A) 40, (B) 20, (C) 10, (D) 5, (E) 3, and (F) 1 °C/min. The mixtures for the DSC were previously annealed at 120 °C for 40 min.

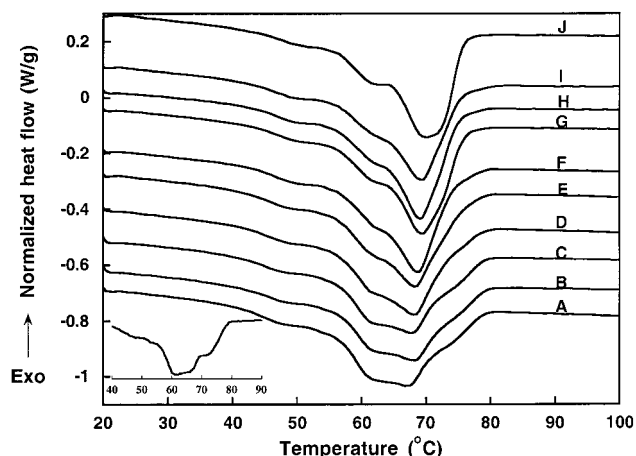


**Figure 5.** DSC thermograms for the mixtures of bentonite and hexadecylamine with amine concentrations at (A) 1.79, (B) 1.84, (C) 1.88, (D) 1.94, (E) 2.22, (F) 2.50, (G) 2.66, (H) 2.84, (I) 3.11, and (J) 3.35 CEC, at a heating rate of 3 °C/min, after they were annealed at 120 °C for 40 min. The inserted figure is the DSC thermogram for the sample with an amine concentration at 1.84 CEC at a heating rate of 1 °C/min.

rate is increased. The superheating of the peak temperature for both transitions is around 7 °C for the change in scanning rate from 1 to 40 °C/min. It is noted that even with a high heating rate of 40 °C/min, the two melting peaks are still discernible, suggesting that they belong to different melting transitions rather than the melting, organization, and remelting processes.

The thermal behavior showed a drastic change as the amine concentration is increased to around 1.8 CEC, as shown in Figure 5. Although the melting transition at 62 °C remains the same, the transition at 75 °C seems to shift to a much lower temperature at 69 °C. Actually, the melting peak at 69 °C consists of two overlapped transitions at 69 and 75 °C, which can be identified on slow heating such as at 1 °C/min, shown in the inserted curve in Figure 5. Therefore, the drastic change of the curve shape between 1.59 and 1.79 CEC is caused by the appearance of a new thermal transition at 69 °C and the significant intensity decrease at 75 °C. As the amine concentration increases further, the intensity of

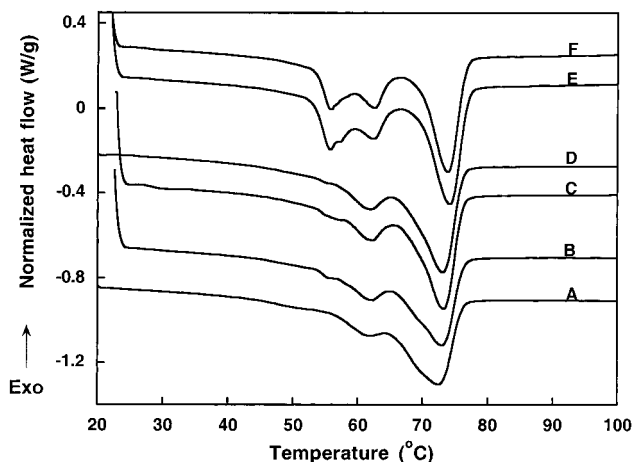


**Figure 6.** DSC thermograms for the mixtures of bentonite and hexadecylamine with amine concentration at (A) 3.85, (B) 4.05, (C) 4.11, (D) 4.35, (E) 5.18, (F) 5.50 CEC, at a heating rate of 3 °C/min, after they were annealed at 120 °C for 40 min.

**Table 1. Comparison of the Results from DSC and X-ray Diffraction**

DSC	Concentration range	0.3-1.6 CEC	1.7-1.9 CEC	2-5 CEC	
	Melting temperature	62 + 75 °C	62 + 69 (newly appears) + 75 °C (becomes weaker and disappears)	62 + 69 °C, 69 °C gradually increases to 75 °C	
X-ray	Concentration range	0.2-0.8 CEC	0.8-1.6 CEC	1.8-4.0 CEC	4.0-6.0 CEC
	d-spacing change	0.29 nm	0.64 nm	1.81 nm	3.91 nm
	Schematic figure				

the transition at 69 °C increases and the peak temperature gradually shifts to higher temperature, with the transition at 75 °C completely disappearing around 1.9 CEC. Finally, two well-resolved transitions with peak temperatures at 62 and 73 °C are observed for samples with amine concentration around 4 CEC, as shown in Figure 6. In the high amine concentration range, the melting transitions are much more symmetric and sharp, reflecting a more homogeneous and well-ordered structure.

The melting behavior of the confined amine is largely dependent on the amine concentration. The trend for the thermal behavior change as a function of amine concentration is generalized in Table 1. Two stable concentration ranges together with a transition range are observed for the melting behavior. Although melting at 62 °C is a common behavior for the samples of all the amine concentrations studied, 75 °C is a unique melting temperature for samples with amine concentration from 0.3 to 1.6 CEC. The peak at 69 °C, which gradually increases to 73 °C, is the unique melting temperature for samples with amine concentration from 2 to 5 CEC. The transition range is around 1.7 to 1.9 CEC, where the old melting transition at 75 °C gradually disappears and the new melting transition at 69 °C appears.

Since the increase of melting temperature is caused by the restriction of amine molecules in the nanoscale

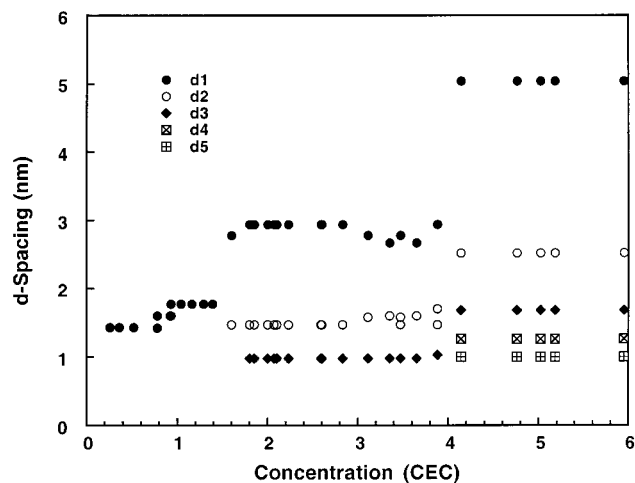


**Figure 7.** The  $d$  spacings of 001 silicate layers obtained from X-ray diffraction results as a function of amine concentration.

confined space, it is quite meaningful to relate the amine melting temperature to the  $d$  spacing of the silicate layers. Figure 7 shows the  $d$  spacing of the silicate layers as a function of amine concentration obtained from X-ray diffraction. The  $d$  spacing and ordering of the silicate layers show a stepwise increase as the amine concentration increases. Based on the basal  $d$  spacing, four concentration ranges are observed as shown in Table 1. For the low concentration range from 0.2 to 1.6 CEC, only the diffraction signal from the 001 silicate layer is observed. A  $d$  spacing increment of 0.29 nm is observed for samples with an amine concentration in the range of 0.2–0.8 CEC, while samples with an amine concentration of 0.8–1.6 CEC have a  $d$  spacing increment of 0.64 nm. The basal  $d$  spacing of the bentonite used for the study is 1.13 nm. For reference, the extended length of hexadecylamine molecules is estimated to be 2.2 nm when calculated using standard bond lengths and angles. The interatomic distance between the farthest two hydrogen atoms of the hexadecylamine molecules is  $0.31 \pm 0.12$  nm. Therefore, for samples with a  $d$  spacing increment of 0.29 nm, the amine chains have no choice but to be lying parallel to the host layers forming a lateral monolayer as depicted in Table 1. Although the amine chains with a  $d$  spacing change of 0.64 nm have the possibility of radiating away from the silicate layers, 0.64 nm being roughly twice the value of 0.29 nm suggests a more possible structure in which the amine chains lie parallel to the host layers forming a lateral bilayer, as shown in Table 1. A  $d$  spacing change of 1.81 nm was observed for samples with amine concentration between 2 and 4 CEC. The sudden large increment in the  $d$  spacing suggests that the amine molecules radiate away from the surface forming an extended (paraffin type) structure with a tilt angle of  $55^\circ$  to the silicate layers. At the same time, the ordering of the silicate layers is significantly improved. Diffraction signals from three orders of silicate layers are observed. For the sample with amine concentration higher than 4 CEC, a  $d$  spacing change of 3.91 nm and diffraction signals from five ordered layers are observed. Again, 3.91 nm being approximately double the value of 1.81 nm suggests that the amine chains in these samples form a two-layer extended (paraffin type) structure with a tilt angle of  $55^\circ$  to the silicate layers. The  $d$  spacing change caused by the neutral amine

chains is the same as that caused by the amine ammonium ions.<sup>5</sup>

By comparison of the results from DSC and X-ray diffraction, as shown in Table 1, common concentration ranges are found as 0.3–1.6 CEC and 2–5 CEC. Therefore, specific amine chain orientation and the melting behavior can be related. For the amine concentration within 0.3–1.6 CEC, the amine chains lie parallel to the silicate layers with the unique melting temperature at  $75^\circ\text{C}$ , while for the amine concentration within 2–5 CEC, the amine chains radiate away from the silicate layers with a tilt angle of  $55^\circ$  with a unique melting temperature at  $69^\circ\text{C}$ . The latter melting temperature gradually increases to  $73^\circ\text{C}$  as more amine is added. Those amine chains that lie parallel to the host layers, which are highly restricted by the silicate surface, exhibit a much higher melting temperature at  $75^\circ\text{C}$ . The amine molecules start to radiate away from the silicate layers around 1.7 CEC and are accompanied by a newly appearing melting transition at  $69^\circ\text{C}$ . A mix of both lateral and paraffin-type structures exist in this transition. Therefore, both of the representative melting temperatures at  $75^\circ\text{C}$  and  $69^\circ\text{C}$  are observed, and the melting transition at  $75^\circ\text{C}$  finally disappears when the lateral structure disappears as amine concentration increases to 1.9 CEC, where all the amine chains radiate away from the silicate layers. Once the amine chains start to radiate away from the silicate layers, the increment of the amine concentration results in close amine chain packing, which results in a gradually increased melting temperature from  $69^\circ\text{C}$  to  $73^\circ\text{C}$ . As can be seen from the X-ray diffraction result, the orientation and organization of the silicate layers change with the adsorption of amine. Integral diffraction signals from one to three and up to five orders are observed as more amine is added, indicating that the amine molecules bring the silicate layers together. This also suggests that the silicate layers go from being poorly ordered structures to being well-ordered structures. Therefore, the common melting transition at  $62^\circ\text{C}$  may be assigned to the melting of amine chains that exist within the poorly ordered silicate layers, which exists in samples of all the amine concentrations.

Assuming that the confined amine has the same heat capacity as the bulk amine, the crystallinity of the confined amine can be calculated, and is shown in Figure 8 as a function of amine concentration. The crystallinity, which is related to the ordering of the confined amine, increases as the amine concentration increases, which is in good agreement with the Fourier transform IR spectroscopic results obtained by Vaia et al.<sup>12</sup> By monitoring frequency shifts of the asymmetric  $\text{CH}_2$  stretching vibrations, they found that the intercalated chains exist in states with varying degrees of order and this order is dependent on the interlayer-packing density and the temperature.<sup>12</sup> However, there are primarily two different increasing rates of the crystallinity for the concentration range studied. When the amine concentration is below 2 CEC, which is the concentration range where the amine chains lie parallel to the silicate layers, the crystallinity increases rapidly and rather linearly. This can be considered to be the result of a rapid increase of amine chain-packing density. The density of hexadecylamine is approximated

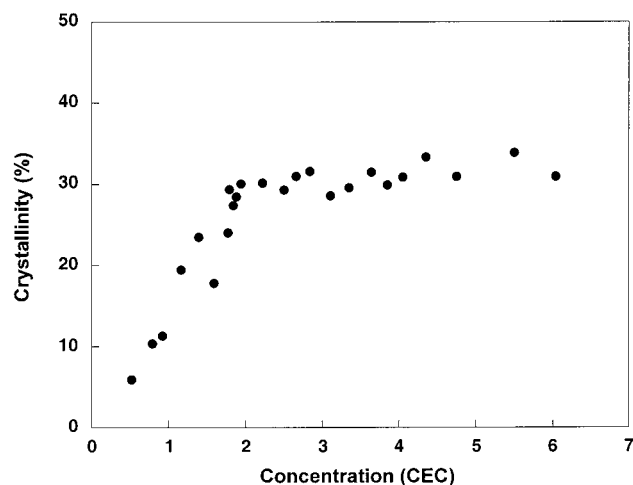


**Figure 8.** Crystallinity of confined amine as a function of amine concentration obtained from the DSC results, assuming that the confined amine has the same heat capacity as the bulk amine.

as  $1 \text{ g/cm}^3$ ; hence, its molecular volume is  $0.40 \text{ nm}^3$ , which yields an area per molecule of  $0.66 \text{ nm}^2$ . The cation-exchange capacity of the clay used is  $80 \text{ meq/100 g}$ . Therefore, the cation density is approximately one charge per  $1.54 \text{ nm}^2$ . This is about twice the area per amine molecule. At a low concentration range, the probability of amine chain overlapping is low, which results in the low crystallinity. The degree of overlapping increases rapidly as amine concentration increases. Since the chains are highly restricted within the silicate layers, the mobility of the chains is very low and no fundamental structure changes could happen in this lateral-packing regime. Therefore, the increased degree of overlapping results in the increased degree of crystallinity while maintaining the melting temperature at  $75 \text{ }^\circ\text{C}$ . When the amine concentration is higher than 2 CEC, the packing is almost saturated, which results in the slow increase in crystallinity. However, the ordering of the chains increases with the amine concentration, so the melting temperature increases gradually. Overall, in the low amine concentration regime, the amine molecules take a more disordered, liquid-like arrangement of chains within the gallery. The ordering of the confined amine is actually low. Even for the highest amine concentration studied here, the crystallinity is about 35%, indicating the existence of a large amount of amine in the noncrystalline phase. This is consistent with the result from the computer simulations in which a not well-ordered, liquid-crystalline-like structure was predicted,<sup>19</sup> although an all-trans conformation was assumed in almost all the previous studies.<sup>5</sup>

To study the influence of polymer chains on the amine fine structure within the silicate layers, the clay and amine mixture with and without a polymer, poly(ethyl methacrylate), were compared by DSC at a heating rate of  $3 \text{ }^\circ\text{C/min}$  as shown in Figure 9. The first heating of the DSC shows similar thermal behavior for the two samples with and without the polymer. The amine intercalation process takes place immediately after the pure amine melting, followed by the crystallization of confined amine, resulting in a higher melting behavior

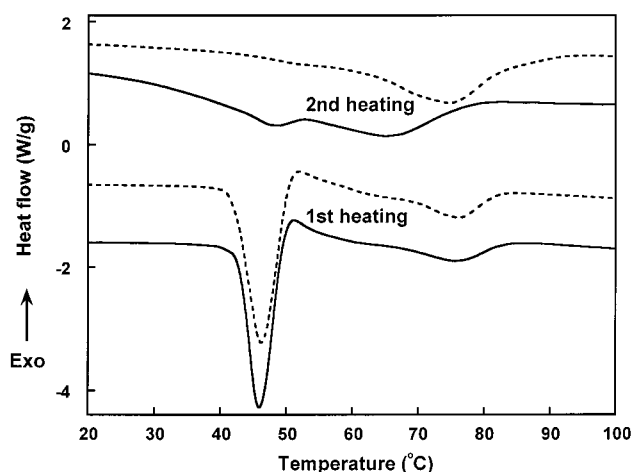


**Figure 9.** DSC thermograms of samples with and without poly(ethyl methacrylate): solid lines; samples with the polymer and dotted lines; samples without the polymer.

**Table 2. Comparison of the Ratio of Reversing Heat Flow over the Total Heat Flow for Bulk Amine and Confined Amine from the TMDSC Results**

amine concn (CEC)	reversible/total (%)	
	bulk amine	intercalated amine
pure amine	11.9	
7.25	13.2	
5.18		32.5
4.35		38.0
2.59		41.2
1.79		31.7
1.29		40.3

than the bulk amine. After the two samples are annealed at  $150 \text{ }^\circ\text{C}$  for 30 min, the second heating of the DSC exhibits a significant difference between the two samples with and without the polymer. For the sample without the polymer, the melting transition of the confined amine is similar to the first heating. However, because the intercalation of the polymer takes place during the annealing, the DSC thermogram of the sample with the polymer is quite different from that without the polymer. The melting temperature is largely decreased, and the area of the transition becomes small. Additionally, even a melting behavior of the bulk amine is observed, indicating that the intercalation of polymer chains may exclude a part of the amine from the silicate layers.

Temperature-modulated DSC can separate the reversing and nonreversing heat flow.<sup>20</sup> Except for a perfect metal crystal, the DSC heat flow of most materials is composed of both reversing and nonreversing components. The ratio between these two components depends on the experimental condition, such as heating rate, and also reflects the ability of the molecules to nucleate. In Table 2, the reversing component over the total heat flow of the bulk amine under a constant heating rate is compared with the amine in the confined space. For the bulk amine, either in the pure amine or in the mixture with the clay (when excess amine is used), the reversing component is around 13% of the total heat flow. On the other hand, the confined amine shows a ratio of the reversing signal as high as 30%. For the confined amine, because of the restriction

(19) Hackett, E.; Manias, E.; Giannelis, E. P. *J. Chem. Phys.* **1998**, *108*, 7410.

(20) Reading, M. *Trends Polym. Sci.* **1993**, *8*, 248.

by the space and, furthermore, by the ion–dipole interaction, the chain conformation is easily maintained and helps to form the nuclei when the temperature is decreased. The high ability of the confined amine to nucleate results in the high ratio of the reversing heat flow.

### Conclusion

DSC provides a new insight into the amine structure within the silicate layers. A strong layering behavior with an ordered amine arrangement is observed. Compared to the traditional nanocomposite study tool of X-ray diffraction, which can only reflect the  $d$  spacing change of the silicate layers, DSC results clearly show the following:

**(1) Amine Intercalation Process.** Amine intercalates into the silicate layers immediately after its melting with a very low energy exchange for this process.

**(2) Fine Structure of Intercalated Amine.** Less than 35% of the confined amine forms an ordered structure within the silicate layers and exhibits a much higher melting temperature than the free amine. Several types of ordered structures are observed for the confined amine, which are largely dependent on the  $d$  spacing of the silicate layers and the amine concentration. The confined amine chains readily nucleate because of their restricted mobility. The ordered structure of amine in the silicate galleries would be influenced by the further intercalation of polymer chains. Further, an important fact is that more than 65% of the nano-scale confined amine does not exhibit the melting transition.

**Acknowledgment.** The authors gratefully acknowledge the financial support of the Federal Aviation Administration (FAA).

CM0103747